

WebWeaver: Breaking Topology Confidentiality in LLM Multi-Agent Systems with Stealthy Context-Based Inference

Zixun Xiong¹, Gaoyi Wu¹, Lingfeng Yao³, Miao Pan³,
Xiaojiang Du¹, Hao Wang¹

¹Department of Electrical and Computer Engineering, Stevens Institute of Technology
²Genentech

³Department of Electrical and Computer Engineering, University of Houston
{zxiong9, gwu13, xdu16, hwang9}@stevens.edu
hi@derek.ma
{lyao12, mpan2}@uh.edu

Abstract

Communication topology is a critical factor in the utility and safety of LLM-based multi-agent systems (LLM-MAS), making it a high-value intellectual property (IP) whose confidentiality remains insufficiently studied. Existing topology inference attempts rely on impractical assumptions, including control over the administrative agent and direct identity queries via jailbreaks, which are easily defeated by basic keyword-based defenses. As a result, prior analyses fail to capture the real-world threat of such attacks. To bridge this realism gap, we propose *WebWeaver*, an attack framework that infers the complete LLM-MAS topology by compromising only a single arbitrary agent instead of the administrative agent. Unlike prior approaches, *WebWeaver* relies solely on agent contexts rather than agent IDs, enabling significantly stealthier inference. *WebWeaver* further introduces a new covert jailbreak-based mechanism and a novel fully jailbreak-free diffusion design to handle cases where jailbreaks fail. Additionally, we address a key challenge in diffusion-based inference by proposing a masking strategy that preserves known topology during diffusion, with theoretical guarantees of correctness. Extensive experiments show that *WebWeaver* substantially outperforms state-of-the-art (SOTA) baselines, achieving about 60% higher inference accuracy under active defenses with negligible overhead.

1 Introduction

LLM-based multi-agent systems (LLM-MASs) have demonstrated expert-level proficiency across scientific (Lu et al., 2024; Schmidgall et al., 2025; Gottweis et al., 2025) and industrial domains (Hong et al., 2023; Kim et al., 2025; Guan et al., 2025), proving highly effective for complex reasoning tasks. Beyond individual agent capabilities, empirical evidence highlights the *communication topology* as a decisive performance factor (Yu et al.,

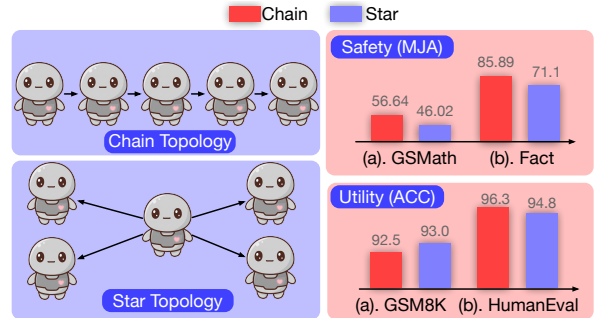


Figure 1: Studies (Yu et al., 2024; Yang et al., 2025) show that communication topology in LLM-MAS significantly affects security and utility performance, with no universally optimal topology, making it a critical form of intellectual property.

2024; Zhang et al., 2025); variations in topology design yield significant disparities in system utility (Zhang et al., 2025; Yang et al., 2025; Cemri et al., 2025) and safety (Zhang et al., 2025) even with identical constituent agents, positioning optimized topologies as high-value intellectual property (IP) as Figure 1 shows. Moreover, prior work indicates that adversaries possessing knowledge of this structure can execute significantly more sophisticated attacks (Shahroz et al., 2025; Wang et al., 2025b) compared to structure-agnostic strategies. Despite these risks, the confidentiality of multi-agent topologies remains underexplored, necessitating a systematic investigation into topology inference attacks to address this critical security gap.

The limited prior work on topology inference suffers from impractical assumptions, leaving the real-world threat of such attacks insufficiently understood. Specifically, previous work assumes that the attacker controls the administrative agent responsible for initiating the system (Wang et al., 2025a). However, this assumption is unrealistic in collaborative LLM-MAS settings where different entities operate different agents (Lu et al., 2024; Schmidgall et al., 2025; Gottweis et al., 2025). In

practice, it is more reasonable to assume that the attacker can compromise a single arbitrary agent rather than the administrative agent. Moreover, existing approaches infer topology by directly querying agent identities via jailbreaks, which can be easily defeated by basic keyword-based defenses.

To address these limitations, we introduce *WebWeaver*, a new attack framework designed to infer LLM-MAS topologies. Distinct from prior works that necessitate control over the system administrator, *WebWeaver* operates by compromising a single arbitrary agent. *WebWeaver* further introduces a covert recursive jailbreak-based mechanism, with a fully jailbreak-free masked diffusion model as a fallback topology completion module. Since they do not need agent IDs and are not based on certain keywords, *WebWeaver* is robust to keyword-based defenses. Additionally, we address a key challenge in the diffusion module by proposing a masking strategy that preserves the known topology during diffusion, with our theoretical guarantees of correctness. Our contributions are as follows:

- We identify a key realism gap in prior topology inference work and propose *WebWeaver*, the first framework to recover complete LLM-MAS topologies by compromising a single arbitrary agent—without requiring administrative privileges or relying on impractical jailbreaks to directly extract neighboring agents’ IDs.
- We also construct a dialogue dataset with explicitly annotated topology, agent prompts, and sender-receiver labels, which facilitates both our study and future research on the security of topology in LLM-MAS.
- We propose a more stealthy attack that infers LLM-MAS topology from agent contexts rather than identifiers, combining a covert recursive jailbreak mechanism with a jailbreak-free diffusion module, and addressing the new challenge of ensuring correctness via a masking strategy that preserves known topology
- Extensive evaluations across diverse datasets demonstrate that *WebWeaver* outperforms state-of-the-art (SOTA) baselines by approximately 60% in inference accuracy under active defenses. Furthermore, both methods maintain negligible overhead, with the jailbreak-free version incurring zero additional computational cost on the target system.

2 Related Works

LLM-MAS Topology. LLM-MASs are collaborative systems in which autonomous agents powered by large language models interact through a communication topology, and they have shown strong performance across scientific and industrial domains (Lu et al., 2024; Schmidgall et al., 2025; Gottweis et al., 2025; Hong et al., 2023; Kim et al., 2025; Guan et al., 2025). Recent studies show that communication topology is critical to system utility and safety, with structural issues leading to concrete failures (Yu et al., 2024; Zhang et al., 2024; Yang et al., 2025; Cemri et al., 2025). As optimized topologies are valuable assets, adversaries with structural knowledge can launch stronger attacks than topology-agnostic ones (Shahroz et al., 2025). However, the confidentiality of multi-agent communication topologies remains largely unexplored.

Vulnerabilities in LLM-MAS. Prior work on LLM-MAS security can be grouped into three categories: system availability, behavioral safety, and topology confidentiality. The first two study denial-of-service attacks, psychological manipulation, and defenses that protect agent behavior and communication (Zhou et al., 2025; Zhang et al., 2024; Chen et al., 2024). The third focuses on inferring the communication topology but remains limited and mainly treats topology leakage as an intellectual property issue (Wang et al., 2025a). Existing approaches in this category rely on unrealistic assumptions, such as direct identity queries via jailbreaks and control over the initiating agent, which rarely hold in collaborative settings (Lu et al., 2024; Schmidgall et al., 2025; Gottweis et al., 2025). Our work falls into the third category and studies topology inference under a realistic threat model based on a single agent and context-based inference.

3 Proposed Methods

3.1 Threat Models

We assume the target LLM-MAS consists of N agents that may be arranged in different topological structures, among which k agents are compromised ($1 \leq k \leq \frac{N}{2}$). We also assume that the system contains no isolated agents, as agents without connections cannot contribute to the LLM-MAS. Thus, we set $k = 1$ in all experiments.

Attacker’s Goal. The attacker aims to infer the communication topology of a target LLM-MAS,

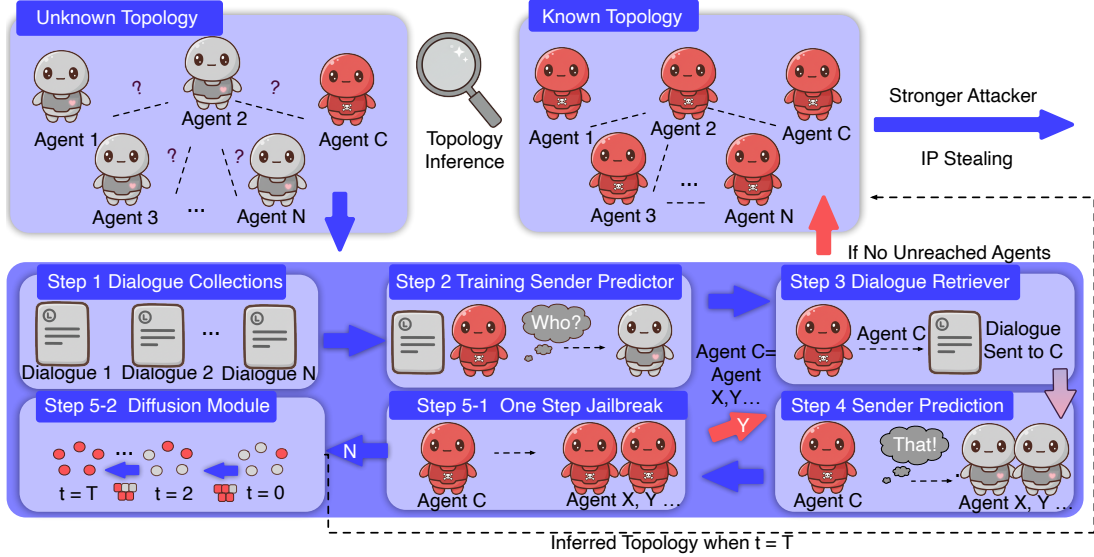


Figure 2: The pipeline of *WebWeaver*: **Step-1**: Inter-agent dialogues are collected offline under known topologies and reused for both training and inference. **Step-2**: The collected dialogues are used to train a sender predictor that infers the sender identity from a received dialogue. **Step-3**: The attacker compromises a selected agent C and retrieves all dialogues received by this agent during interaction. **Step-4**: The trained sender predictor is applied to the retrieved dialogues to infer the set of agents directly connected to the selected agent. **Step-5**: If the initial or optimized jailbreak succeeds (denoted as Y), the attacker uses it to induce connected agents to request additional context and iteratively repeats dialogue retrieval and sender prediction to expand the inferred graph until no new agents are uncovered; if the optimized jailbreak still fails (denoted as N), the attacker performs topology completion using a masked diffusion model (i.e., DDPM) trained on the collected dialogues and conditioned on the partially known topology to infer the complete interaction structure.

which is a high-value intellectual property of its owner. Knowledge of the topology also enables the attacker to better understand agent coordination and to launch stronger downstream attacks (Shahroz et al., 2025; Wang et al., 2025b). This objective naturally arises in collaborative settings such as inter-university research (Lu et al., 2024; Schmidgall et al., 2025; Gottweis et al., 2025), where institutions deploy their own agents and interact through shared tasks. In such scenarios, an institution may infer the topology of the target LLM-MAS from observed interactions. As a result, it can steal the intellectual property of the LLM-MAS owner and deploy more advanced attacks to access the private data of other agents.

Attacker’s Ability. We consider a realistic attacker whose capabilities are consistent with the example. First, the attacker controls a single arbitrary agent in the target LLM-MAS and can proactively request context from adjacent agents. This behavior is reasonable in practice, as agents often operate on different devices and may request context retransmission due to asynchronous execution or temporary disconnections. Second, the attacker knows which agents participate in the target

LLM-MAS and can collect inter-agent dialogues using a separate LLM-MAS under its own control. For example, in collaborations between universities, each institution may host its own agent specialized in a particular domain. A university focusing on Domain A may operate its own LLM-MAS to collaborate with other universities and record dialogue exchanges during joint research activities (Lu et al., 2024; Schmidgall et al., 2025; Gottweis et al., 2025). These collected dialogues can then be leveraged to infer the communication topology of another LLM-MAS deployed by a different university specializing in Domain B, thereby achieving the attacker’s goal.

Challenges and Contributions. 1). Topology inference in LLM-MAS often relies on explicitly querying agent IDs, which is easily defeated by keyword-based defenses; we instead propose a training-based framework that infers topology purely from contextual signals inherent in multi-agent collaboration, eliminating the need for identifier queries. 2). Existing jailbreak strategies are largely static and thus detectable in multi-agent settings; we introduce an adaptive jailbreak that dynamically adjusts its prompts, achieving substan-

tially higher stealthiness under adaptive defenses. 3). When jailbreaks fail, topology inference reduces to a zero-shot, NP-hard graph completion problem (Fang et al., 2025); we model this setting as diffusion-based graph reconstruction using dynamic dialogues, while addressing the new challenges of structural consistency to preserve known topology during inference.

3.2 Jailbreak-based Module

Data Collection & Sender Predictor Training.

The extraction process begins by passively collecting interaction logs from the compromised LLM-MAS environment as discussed in Figure 2. We compile a dataset of dialogue history \mathcal{H} , where each entry consists of message content and the associated sender identity. For example, a log sequence might appear as: $\{sender: Agent A, receiver: Agent B, dialogue: "XXX"\}$. Using this labeled dataset¹, we train a sender predictor, S_θ , to learn the distinct linguistic fingerprints and role-specific syntax of different agents. The predictor is optimized to map a message content snippet m to a specific agent identity s , maximizing the probability: $P_\theta(sender = s|m)$. This allows us to de-anonymize the source of a message based purely on its semantic content.

Dialogue Retrieval & Sender Prediction. Once trained, we deploy the S_θ in conjunction with a compromised agent, denoted as A_C . This agent acts as a listener within the graph. As A_C receives incoming messages from its immediate neighbors during standard system operation, it feeds these dialogue fragments into S_θ . For every received message m_i , the predictor outputs the most probable sender identity: $\hat{s} = \arg \max_s S_\theta(m_i)$. By aggregating these predictions over time, A_C effectively infers its local adjacency matrix \mathbf{A}_{obs} , identifying all agents A_i such that a direct edge (A_i, A_C) exists, solely by analyzing the “voice” of the incoming traffic.

Recursive Jailbreak. To expand this discovery from the local neighborhood to the whole graph, we implement a recursive jailbreak mechanism. We inject a “propagation prompt” into A_C , instructing it to command its neighbors to: 1). forward their own conversation histories (without the sender index) back to A_C , and 2). repeat this command to *their* neighbors. This creates a cascade of con-

text leakage, allowing us to recursively infer the global topology with the help of the sender predictor. However, if neighbors are equipped with safety filters that reject this instruction, we escalate to an optimization-based attack. We employ a greedy coordinate gradient (GCG) approach using a local proxy LLM. Since we lack white-box access to the victim agents, we calculate gradients on the local model to optimize an adversarial suffix that maximizes the likelihood of compliance. To formalize this, we define the optimization objective as minimizing the negative log-likelihood of the target response:

$$\min_{\delta} \mathcal{L}(\delta) = - \sum_{t=1}^{|\mathcal{P}|} \log p(y_t | \mathbf{x}_{prop} \oplus \delta), \quad (1)$$

where y_t is a sentence that starts with “Sure”, x is the original “propagation prompt”, δ is the suffix we want to optimize, and \oplus is the concatenation operation. We solve this using the GCG method by computing gradients with respect to token embeddings of δ : $\nabla_{\delta_i} \mathcal{L}$ for $i = 1, \dots, |\delta|$. Finally, we iteratively update the suffix by selecting the best candidate from the top- k substitutions. This optimized suffix is then transferred to the target system. By iteratively refining the prompt until it bypasses the defense, we force the neighbors to execute the propagation command, eventually retrieving the global context and revealing the entire network structure \hat{G} . The complete procedure is summarized in the Appendix.

3.3 Jailbreak-free Diffusion Module

We also propose a diffusion-based module to infer the global topology of the target LLM-MAS when jailbreak is infeasible. We draw inspiration from diffusion models, which are fundamentally designed for denoising. Moreover, our task can be viewed as a graph completion problem, where topology inference naturally corresponds to denoising a partially observed interaction graph. We also address a key challenge in applying DDPMs, namely that standard diffusion processes cannot preserve known topology; to resolve this, we introduce a masking module, as described later.² Since we collect a set of interaction topologies and associated dialogues that can be used for training, we model topology inference as a diffusion process,

¹We will release the dataset recently.

²The proof of why our masking can be applied without violating the properties of DDPM is provided in the Appendix.

enabling effective inference (stealing) of the underlying interaction topology. Thus, only Steps 1 and 2 in Figure 2 are required when combined with the diffusion model, eliminating the need for jailbreak.

Problem Formulation. We represent the LLM-MAS topology as an undirected graph $\mathcal{G} = (\mathcal{V}, \mathcal{E})$, characterized by a symmetric adjacency matrix $\mathbf{A} \in \{0, 1\}^{N \times N}$ describing both vertices (i.e., agents) V and edges E , where N denotes the number of agents. We also consider a scenario of partial observability where connections for a subset of agents are known³: Let $\mathbf{M} \in \{0, 1\}^{N \times N}$ be a binary mask matrix, where $M_{ij} = 1$ indicates that the relationship between agent i and agent j is observed, and $M_{ij} = 0$ indicates an unknown status. Given the observed partial topology $\mathbf{A}_{obs} = \mathbf{A}_{gt} \odot \mathbf{M}$, our goal is to infer the ground-truth topology \mathbf{A}_{gt} by inferring the missing entries in $(\mathbf{1} - \mathbf{M}) \odot \mathbf{A}_{gt}$, where \odot denotes the Hadamard product.

Diffusion-based Topology Inference Generative Model. The aforementioned problem can be addressed using a diffusion model: the observed subgraph is treated as a noisy input \mathbf{A}_{obs} , while the ground-truth graph corresponds to the clean signal \mathbf{A}_{gt} . Since diffusion models are designed to denoise corrupted inputs, they can be leveraged to recover \mathbf{A}_{gt} too. All we need to do in this part is to model the forward and reverse processes of the diffusion model. Specifically, we employ a denoising diffusion probabilistic model (DDPM) to learn the distribution of target topology, where $\mathbf{x}_0 = \mathbf{A}_{gt}$. The forward process is a Markov chain that gradually adds Gaussian noise to the data according to a variance schedule β_1, \dots, β_T :

$$q(\mathbf{x}_t | \mathbf{x}_{t-1}) = \mathcal{N}(\mathbf{x}_t; \sqrt{1 - \beta_t} \mathbf{x}_{t-1}, \beta_t \mathbf{I}). \quad (2)$$

The reverse process learns to denoising the graph structure by predicting the noise $\epsilon_\theta(\mathbf{x}_t, t)$ to approximate the posterior $q(\mathbf{x}_{t-1} | \mathbf{x}_t)$. The sampling step is defined as:

$$\mathbf{x}_{t-1} = \frac{1}{\sqrt{\alpha_t}} \left(\mathbf{x}_t - \frac{1 - \alpha_t}{\sqrt{1 - \alpha_t}} \epsilon_\theta(\mathbf{x}_t, t) \right) + \sigma_t \mathbf{z}, \quad (3)$$

where $\alpha_t = 1 - \beta_t$, $\bar{\alpha}_t = \prod_{i=1}^t \alpha_i$, and $\mathbf{z} \sim \mathcal{N}(\mathbf{0}, \mathbf{I})$.

³This is done by Step 2 and Step 3

Topology Inference via Subgraph Guidance.

Before applying the above DDPM for graph completion, a key challenge arises: directly using DDPM would inevitably corrupt the known subgraph (the observed topology). To address this issue, we introduce a *Masked Topology Inpainting* strategy during the reverse sampling phase. Standard unconditional sampling may generate valid topologies that are inconsistent with the observed nodes. To enforce consistency, we fuse the model’s prediction with the observed ground truth at each denoising step.

Specifically, at each reverse step $t - 1$, we obtain the model’s prediction \mathbf{x}_{t-1}^{pred} using Equation (3). Simultaneously, we compute the noisy state of the observed data, denoted as \mathbf{x}_{t-1}^{obs} , by sampling from the forward process marginal $q(\mathbf{x}_{t-1} | \mathbf{x}_0)$ using the known \mathbf{A}_{obs} ⁴:

$$\mathbf{x}_{t-1}^{obs} \sim \mathcal{N}(\sqrt{\bar{\alpha}_{t-1}} \mathbf{A}_{obs}, (1 - \bar{\alpha}_{t-1}) \mathbf{I}).$$

Critically, we inject the known information into the sampling trajectory using the mask \mathbf{M} :

$$\mathbf{x}_{t-1} = (\mathbf{1} - \mathbf{M}) \odot \mathbf{x}_{t-1}^{pred} + \mathbf{M} \odot \mathbf{x}_{t-1}^{obs}.$$

This operation ensures that the known subgraph region follows the correct noise trajectory grounded in \mathbf{A}_{obs} , while the diffusion model fills in the masked regions $(\mathbf{1} - \mathbf{M})$ to form a coherent global structure. After T epochs, we can derive the predicted topology. The complete procedure is summarized in Algorithm 2.

4 Evaluation

Datasets & Models We evaluate our framework on four diverse datasets. CSQA (Talmor et al., 2019) contains 12,247 multiple-choice questions requiring commonsense reasoning over ConceptNet, while GSM8k (Cobbe et al., 2021) includes 8,500 grade-school math problems that test multi-step logical deduction. Fact (Yu et al., 2024) is a synthetic dataset of indisputable factual statements generated via GPT-4 to evaluate information fidelity, and Bias (Yu et al., 2024) consists of stereotype-based statements designed to assess safety and alignment within agent topologies. We consider four representative models: Llama 3.1

⁴Directly injecting clean ground-truth data would cause a distribution shift, as the model expects noisy inputs at intermediate steps. Equation (3) ensures the known subgraph carries the correct noise level corresponding to timestep $t - 1$, maintaining consistency with the diffusion trajectory.

8B (Dubey et al., 2024), Qwen 2.5 7B (Team, 2024b), Mistral NeMo 12B (AI and NVIDIA, 2024), and Gemma 2 9B (Team, 2024a). For each experiment, a single model is uniformly assigned to all agents, and final results are averaged over multiple LLM-MAS configurations spanning all four models.

Agents and LLM-MAS. For each agent, there’s a different prompt for their roles⁵. Considering previous work encourages different roles and model heterogeneity (Lu et al., 2024; Schmidgall et al., 2025; Gottweis et al., 2025), our design is practical.

Baselines. To ensure that our results are representative, in addition to directly comparing with the only baseline (Wang et al., 2025a) that is directly relevant to our task, we also include the most recent optimization-based graph completion method. Specifically, we adopt CZRL (Fang et al., 2025), which infers the entire topology directly from the observed nodes and edges using a model trained on collected data (we assume the attacker can access dialogues from other agents via the jailbreak and use dialogues to learn the text embeddings of each node).

Metrics. We use mean reciprocal rank (MRR) to evaluate the accuracy of the attacker in inferring the underlying LLM-MAS communication topology. For each agent, the attacker ranks all candidate agents as potential neighbors, and MRR measures how highly the true connected agents are ranked in this list. This metric is well-suited for topology inference since it directly reflects the quality of the predicted ranking rather than a single hard decision. A higher MRR indicates that the attacker consistently prioritizes true communication links, demonstrating more accurate topology recovery. We further report Precision, Recall, and F1 Score to evaluate the accuracy of both the sender predictor and the subsequent graph completion results. Precision measures the fraction of predicted senders or inferred links that are correct, while Recall quantifies the coverage of true senders or communication links recovered by the attacker. The F1-score provides a balanced assessment by jointly considering precision and recall, which is critical in the presence of class imbalance and multiple candidate agents. Together, these metrics complement ranking-based evaluation by characterizing

⁵For details of the prompts, please refer to the appendix.

Dataset	Precision	Recall	F1 Score
CSQA	0.8794	0.8773	0.8772
GSM8k	0.9471	0.9472	0.9470
Fact	0.9606	0.9597	0.9597
Bias	0.9830	0.9830	0.9830

Table 1: Sender predictor performance across different datasets.

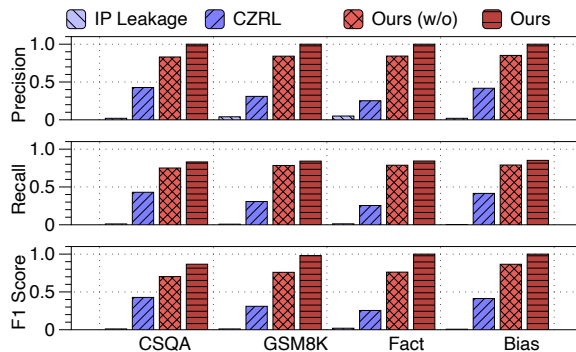


Figure 3: Robustness of different attacks against a keyword-based defense that rejects any request containing information intended to reveal adjacent agent IDs. “Ours (w/o)” is the jailbreak-free module of *WebWeaver*, and “Ours” is the jailbreak-based *WebWeaver*.

the correctness of discrete sender identification and topology inference.

4.1 Main Results

Sender Prediction. To demonstrate that our sender predictor can successfully identify the sender of the given dialogue, we examine Precision, Recall, and F1 Score averaged over all dialogue traces across four different datasets. As shown in Table 1, our sender predictors achieve consistently strong performance across all four datasets, demonstrating their ability to effectively distinguish among different agents. This indicates that agents exhibit distinct behavioral or stylistic identities, which are implicitly reflected in their generated dialogues. As a result, the sender predictor can

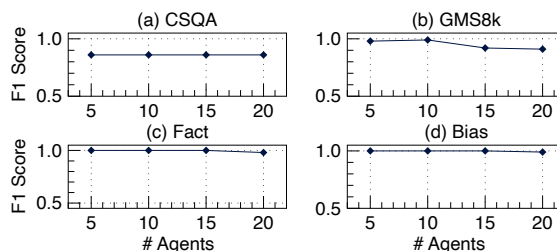


Figure 4: Scalability of the jailbreak-based module with different numbers of agents.

Dataset	Jailbreak-based module				Jailbreak-free module			
	Precision	Recall	F1 Score	MRR	Precision	Recall	F1 Score	MRR
CSQA	1.0000	0.7688	0.8666	0.7292	0.8310	0.7506	0.7887	0.7029
GSM8k	1.0000	0.9688	0.9821	0.9208	0.8418	0.7844	0.8120	0.7593
Fact	1.0000	1.0000	1.0000	1.0000	0.8432	0.7876	0.8145	0.7618
Bias	1.0000	1.0000	1.0000	1.0000	0.8518	0.7902	0.8198	0.8659

Table 2: Graph completion performance under jailbreak-based and jailbreak-free modules of *WebWeaver*.

successfully learn discriminative patterns from dialogue content alone, enabling accurate sender identification. Overall, the performance is robust, with all datasets achieving F1 scores above 0.85, highlighting the reliability of the proposed predictor. We also observe that CSQA yields comparatively lower scores than the other datasets, likely due to its more diverse reasoning paths and less consistent dialogue patterns. In contrast, datasets such as GSM8k, Fact, and Bias exhibit more structured or homogeneous dialogue characteristics, making agent-specific features easier to capture and leading to higher prediction accuracy.

Graph Completion. To demonstrate the effectiveness of our graph completion capability, we evaluate the performance of topology inference under both jailbreak-based and jailbreak-free modules, as reported in Table 2. Overall, both modules achieve strong results across all datasets, indicating that the proposed graph completion strategy is effective even without relying on jailbreak capabilities. The jailbreak-based module consistently attains higher precision and F1 scores, in some cases reaching perfect performance, suggesting that direct context access provides more complete and reliable neighborhood information for topology inference. In contrast, the jailbreak-free module exhibits a moderate performance drop, particularly on CSQA, but still maintains competitive F1 scores above 0.78 across all datasets. This demonstrates that our approach remains robust in more restrictive settings, and that sufficient structural signals can be inferred from local topology alone. The relatively larger gap on CSQA can be attributed to its higher reasoning diversity and noisier interaction patterns leading to the performance degradation of the sender predictor, whereas more structured datasets such as GSM8k, Fact, and Bias facilitate more accurate graph inference. A few inference samples of the jailbreak-free module are shown in Figure 5.

Robustness against Potential Defenses. Figure 3 illustrates the robustness of different attack strategies against filtering-based defenses, where the sender agent’s index is filtered from the communication. As observed, the IP Leakage baseline exhibits near-zero performance across all metrics; this collapse is expected, as the method relies exclusively on explicit agent indices, which are effectively neutralized by the filter. While CZRL maintains moderate performance, it remains sub-optimal because it fails to fully exploit the compromised agent’s capability to intercept incoming dialogues and actively disseminate messages to neighbors. In contrast, our approach demonstrates superior resilience. Even our jailbreak-free module (“Ours (w/o)”) outperforms the SOTA by inferring topology solely through dialogue context. However, the complete method (Ours) achieves the highest precision and recall. This performance gap attributes to the jailbreak mechanism, which enables active, recursive probing of the network structure, whereas the ablation is limited to inferring immediate adjacencies via passive dialogue analysis. Thus, in practice, we adopt an adaptive strategy: we initially deploy the jailbreak-based module and fall back to the jailbreak-free counterpart only if the jailbreak remains unsuccessful after multiple rounds of suffix optimization via Equation (1).

4.2 Scalability

To evaluate the robustness and scalability of our proposed attack, we measured its performance across varying system sizes in Figure 4, specifically scaling the number of agents from 5 to 20.⁶ As illustrated in Figure 3, the attack maintains consistently high F1 scores across all four benchmarks (CSQA, GSM8k, Fact, and Bias), demonstrating that the attack effectiveness does not degrade as the agent network expands. It is important to note that existing works on LLM-MAS and practical deployments of LLM-based expert systems typically

⁶The scalability of model sizes is provided in the Appendix.

Dataset	IP Leakage		WebWeaver		w/o	
	Off.	On.	Off.	On.	Off.	On.
CSQA	N/A	25.3	50.4	30.7	35.2	N/A
GSM8K	N/A	32.0	43.1	35.8	34.6	N/A
Fact	N/A	8.6	39.4	12.7	16.1	N/A
Bias	N/A	9.9	54.4	15.4	15.1	N/A

Table 3: Overall overhead analysis. All measurements are reported in seconds. “w/o Jailbreak” is when only the jailbreak-free module is activated.

Predictor	CSQA	GSM8K	Fact	Bias
Fixed	0.64	0.56	0.69	0.58
Ours	0.72	0.93	1.00	1.00

Table 4: Ablation of jailbreak prompts. We report graph completion F1 when benign agents use LLaMa Guard (Inan et al., 2023) prompted by a single jailbreak example. “Fixed” uses the initial prompt, while “Ours” uses the optimized prompt.

employ a concise topology ranging from 2 to 10 agents (Lu et al., 2024; Schmidgall et al., 2025; Gottweis et al., 2025; Kim et al., 2025). Consequently, our experimental setting, which extends up to 20 agents, not only fully encompasses the standard operating range of current practical applications but also significantly exceeds it. This empirical evidence confirms that our evaluation is sufficient and that the attack remains potent even in substantially scaled-up environments.

4.3 Performance Analysis

To assess computational feasibility, Table 3 reports offline training costs and online runtime overhead. Results show that the jailbreak-free module achieves runtime comparable to the baseline, while fully eliminating online overhead by operating passively, thereby preserving original system workflows and maximizing stealthiness. Although the jailbreak-based module incurs higher computation than the baseline (with CZRL overhead similar to the jailbreak-free variant), this cost is justified by its substantially higher topology inference accuracy (Figure 3). Moreover, the attack’s minimal online footprint is naturally obscured by the inherent stochasticity of LLM generation. Finally, although these results reflect local limits, stronger backends make latency negligible, and offline overhead is incurred only once.

Prediction	CSQA	GSM8K	Fact	Bias
Logistic	.5/.6/.5	.5/.7/.6	.5/.8/.6	.5/.6/.5
BERT	.8/.8/.8	.9/.9/.9	.9/.9/.9	.9/.1/.9
Ours	.8/.8/.8	.9/.9/.9	.9/.9/.9	.9/.9/.9

Table 5: Ablation study of sender predictors. Each cell reports Precision, Recall, and F1 score in the format Precision/Recall/F1 score.

5 Ablation Studies

Sender Predictor. We conducted an ablation study on three representative sender predictors: a logistic baseline, a BERT-based encoder, and our proposed approach. While deep learning-based models (e.g., BERT) can offer marginal performance gains, we selected our proposed method as the default setting because it is gradient-free and significantly minimizes computational overhead. Consequently, our approach ensures high efficiency without sacrificing substantial accuracy. However, we note that in resource-abundant scenarios, employing heavier encoders, such as BERT or LLMs, could further elevate attack success rate.

Jailbreak Prompt Optimization. To evaluate robustness against active defenses, we deploy LLaMA Guard (Inan et al., 2023) as a safety auditor and conduct an ablation comparing a static “Fixed” prompt with our GCG-based adaptive jailbreak. As shown in Table 4, the adaptive method substantially outperforms the baseline, achieving near-perfect F1 on Fact and Bias benchmarks, demonstrating the effectiveness of gradient-based optimization in bypassing safety guardrails. Incorporating newer SOTA jailbreak methods may further improve attack success.

6 Conclusion

In this paper, we advance LLM-MAS security with *WebWeaver*, the first topology inference framework operable under single-agent compromise that is robust to keyword-based defense. Unlike prior works limited by impractical assumptions, *WebWeaver* employs an adaptive dual-strategy integrating covert jailbreaks with structurally consistent diffusion to evade detection. Evaluations show a 60% accuracy improvement with negligible overhead, highlighting the inadequacy of keyword-based defenses and the need for topology-aware protections.

Limitations

Due to ethical and practical considerations, we do not evaluate our approach on real-world online academic collaboration platforms or live collaborative projects. Conducting such experiments would require interacting with human participants and potentially sensitive research workflows, raising nontrivial concerns regarding consent, privacy, and unintended interference with ongoing collaborations. Moreover, deploying our method in these settings would necessitate substantial domain-specific background knowledge and close coordination with active research teams, which goes beyond the intended scope of this paper. As a result, our evaluation is limited to controlled and reproducible experimental settings. We view this as an important direction for future work and plan to collaborate with researchers from different disciplines to design ethically sound, consent-aware, and context-informed studies that can assess the applicability and impact of our method in real-world collaborative environments.

References

- Mistral AI and NVIDIA. 2024. Mistral nemo: our new best small model. <https://mistral.ai/news/mistral-nemo/>.
- Mert Cemri, Melissa Z Pan, Shuyi Yang, Lakshya A Agrawal, Bhavya Chopra, Rishabh Tiwari, Kurt Keutzer, Aditya Parameswaran, Dan Klein, Kannan Ramchandran, and 1 others. 2025. Why do multi-agent llm systems fail? *arXiv preprint arXiv:2503.13657*.
- Bei Chen, Gaolei Li, Xi Lin, Zheng Wang, and Jianhua Li. 2024. Blockagents: Towards byzantine-robust llm-based multi-agent coordination via blockchain. In *Proceedings of the ACM Turing Award Celebration Conference-China 2024*, pages 187–192.
- Karl Cobbe, Vineet Kosaraju, Mohammad Bavarian, Mark Chen, Heewoo Jun, Lukasz Kaiser, Matthias Plappert, Jerry Tworek, Jacob Hilton, Reiichiro Nakano, and 1 others. 2021. Training verifiers to solve math word problems. *arXiv preprint arXiv:2110.14168*.
- Abhimanyu Dubey, Abhinav Jauhri, Abhinav Pandey, Ashutosh Kadian, Ahmad Al-Dahle, Aiesha Letman, Akhil Mathur, Schelten Schelten, Amy Yang, Angela Fan, and 1 others. 2024. The llama 3 herd of models. *arXiv preprint arXiv:2407.21783*.
- Zhiyi Fang, Hang Yu, Changhua Xu, Zhuofeng Li, Jie Ying, and Shaorong Xie. 2025. Contrastive zero-shot relational learning for knowledge graph completion. *Knowledge-Based Systems*, page 113425.
- Juraj Gottweis, Wei-Hung Weng, Alexander Daryin, Tao Tu, Anil Palepu, Petar Sirkovic, Artiom Myaskovsky, Felix Weissenberger, Keran Rong, Ryutarō Tanno, and 1 others. 2025. Towards an ai co-scientist. *arXiv preprint arXiv:2502.18864*.
- Xinyu Guan, Li Lina Zhang, Yifei Liu, Ning Shang, Youran Sun, Yi Zhu, Fan Yang, and Mao Yang. 2025. rstar-math: Small llms can master math reasoning with self-evolved deep thinking. *arXiv preprint arXiv:2501.04519*.
- Sirui Hong, Mingchen Zhuge, Jonathan Chen, Xiawu Zheng, Yuheng Cheng, Jinlin Wang, Ceyao Zhang, Zili Wang, Steven Ka Shing Yau, Zijuan Lin, and 1 others. 2023. Metagpt: Meta programming for a multi-agent collaborative framework. In *The Twelfth International Conference on Learning Representations*.
- Hakan Inan, Kartikeya Upasani, Jianfeng Chi, Rashi Rungta, Krithika Iyer, Yuning Mao, Michael Tontchev, Qing Hu, Brian Fuller, Davide Testuggine, and 1 others. 2023. Llama guard: Llm-based input-output safeguard for human-ai conversations. *arXiv preprint arXiv:2312.06674*.
- Taesoo Kim, HyungSeok Han, Soyeon Park, Dae R Jeong, Dohyeok Kim, Dongkwan Kim, Eunsoo Kim, Jiho Kim, Joshua Wang, Kangsu Kim, and 1 others. 2025. Atlantis: Ai-driven threat localization, analysis, and triage intelligence system. *arXiv preprint arXiv:2509.14589*.
- Chris Lu, Cong Lu, Robert Tjarko Lange, Jakob Foerster, Jeff Clune, and David Ha. 2024. The ai scientist: Towards fully automated open-ended scientific discovery. *arXiv preprint arXiv:2408.06292*.
- Samuel Schmidgall, Yusheng Su, Ze Wang, Ximeng Sun, Jialian Wu, Xiaodong Yu, Jiang Liu, Zicheng Liu, and Emad Barsoum. 2025. Agent laboratory: Using llm agents as research assistants. *arXiv preprint arXiv:2501.04227*.
- Rana Shahroz, Zhen Tan, Sukwon Yun, Charles Fleming, and Tianlong Chen. 2025. Agents under siege: Breaking pragmatic multi-agent llm systems with optimized prompt attacks. In *Proceedings of the 63rd Annual Meeting of the Association for Computational Linguistics (Volume 1: Long Papers)*, pages 9661–9674.
- Alon Talmor, Jonathan Herzig, Nicholas Lourie, and Jonathan Berant. 2019. Commonsenseqa: A question answering challenge targeting commonsense knowledge. In *Proceedings of the 2019 Conference of the North American Chapter of the Association for Computational Linguistics: Human Language Technologies, Volume 1 (Long and Short Papers)*, pages 4149–4158.
- Gemma Team. 2024a. Gemma 2: Improving open language models at a practical size. *arXiv preprint arXiv:2408.00118*.

Qwen Team. 2024b. Qwen2.5 technical report. *arXiv preprint arXiv:2412.15115*.

Liwen Wang, Wenxuan Wang, Shuai Wang, Zongjie Li, Zhenlan Ji, Zongyi Lyu, Daoyuan Wu, and Shing-Chi Cheung. 2025a. Ip leakage attacks targeting llm-based multi-agent systems. *arXiv preprint arXiv:2505.12442*.

Shilong Wang, Guibin Zhang, Miao Yu, Guancheng Wan, Fanci Meng, Chongye Guo, Kun Wang, and Yang Wang. 2025b. G-safeguard: A topology-guided security lens and treatment on llm-based multi-agent systems. *arXiv preprint arXiv:2502.11127*.

Jiaxi Yang, Mengqi Zhang, Yiqiao Jin, Hao Chen, Qingsong Wen, Lu Lin, Yi He, Srijan Kumar, Weijie Xu, James Evans, and 1 others. 2025. Topological structure learning should be a research priority for llm-based multi-agent systems. *arXiv preprint arXiv:2505.22467*.

Miao Yu, Shilong Wang, Guibin Zhang, Junyuan Mao, Chenlong Yin, Qijiong Liu, Qingsong Wen, Kun Wang, and Yang Wang. 2024. Netsafe: Exploring the topological safety of multi-agent networks. *arXiv preprint arXiv:2410.15686*.

Hangfan Zhang, Zhiyao Cui, Jianhao Chen, Xinrun Wang, Qiaosheng Zhang, Zhen Wang, Dinghao Wu, and Shuyue Hu. 2025. Stop overvaluing multi-agent debate—we must rethink evaluation and embrace model heterogeneity. *arXiv preprint arXiv:2502.08788*.

Zaibin Zhang, Yongting Zhang, Lijun Li, Jing Shao, Hongzhi Gao, Yu Qiao, Lijun Wang, Huchuan Lu, and Feng Zhao. 2024. Psysafe: A comprehensive framework for psychological-based attack, defense, and evaluation of multi-agent system safety. In *Proceedings of the 62nd Annual Meeting of the Association for Computational Linguistics (Volume 1: Long Papers)*, pages 15202–15231.

Zhenhong Zhou, Zherui Li, Jie Zhang, Yuanhe Zhang, Kun Wang, Yang Liu, and Qing Guo. 2025. Corba: Contagious recursive blocking attacks on multi-agent systems based on large language models. *arXiv preprint arXiv:2502.14529*.

A Appendix

A.1 Theoretical Analysis

In this section, we analyze the theoretical validity of the *Manifold-Constrained Fusion* mechanism employed in the Jailbreak-free Module (Algorithm 2). We formally prove that replacing the observed sub-graph components during the reverse diffusion process constitutes a legitimate sampling strategy for the conditional posterior $p(\mathbf{x}_{unseen}|\mathbf{x}_{seen})$.

Problem Setup. Let $\mathbf{x} \in \mathbb{R}^N$ denote the vectorized graph topology. We partition \mathbf{x} using a binary mask $\mathbf{M} \in \{0, 1\}^N$ into observed components $\mathbf{x}_o = \mathbf{M} \odot \mathbf{x}$ and unobserved components $\mathbf{x}_u = (\mathbf{1} - \mathbf{M}) \odot \mathbf{x}$. The reverse-time SDE for the unconditional marginal $p_t(\mathbf{x})$ is given by $d\mathbf{x} = [\mathbf{f}(\mathbf{x}, t) - g^2(t)\nabla_{\mathbf{x}} \log p_t(\mathbf{x})]dt + g(t)d\bar{\mathbf{w}}$.

Theorem 1. *Assuming the learned score function $\epsilon_\theta(\mathbf{x}_t, t) \approx -\sigma_t \nabla_{\mathbf{x}_t} \log p_t(\mathbf{x}_t)$ is accurate, the Manifold-Constrained Fusion step (Algorithm 2, Lines 11-14) generates samples that converge to the true conditional posterior $p(\mathbf{x}_u|\mathbf{x}_o)$ as the number of discretization steps $T \rightarrow \infty$.*

Proof. The proof relies on decomposing the score function over the orthogonal subspaces defined by \mathbf{M} . Consider the gradient of the joint log-density with respect to the unobserved variables \mathbf{x}_u :

$$\nabla_{\mathbf{x}_u} \log p_t(\mathbf{x}_u, \mathbf{x}_o) = \nabla_{\mathbf{x}_u} \log p_t(\mathbf{x}_u|\mathbf{x}_o) + \underbrace{\nabla_{\mathbf{x}_u} \log p_t(\mathbf{x}_o)}_{=0}. \quad (4)$$

Since the marginal distribution of the observed part $p_t(\mathbf{x}_o)$ is independent of \mathbf{x}_u , the second term vanishes. This implies the identity:

$$(\mathbf{1} - \mathbf{M}) \odot \nabla_{\mathbf{x}} \log p_t(\mathbf{x}) = \nabla_{\mathbf{x}_u} \log p_t(\mathbf{x}_u|\mathbf{x}_o). \quad (5)$$

Substituting this into the reverse SDE governing \mathbf{x}_u , we obtain:

$$d\mathbf{x}_u = [\mathbf{f}(\mathbf{x}_u, t) - g^2(t)\nabla_{\mathbf{x}_u} \log p_t(\mathbf{x}_u|\mathbf{x}_o)]dt + g(t)d\bar{\mathbf{w}}_u. \quad (6)$$

This is precisely the Langevin dynamic required to sample from the conditional distribution. Algorithm 2 implements a numerical Euler-Maruyama integration of this system. Specifically, the fusion step $\mathbf{x}_{t-1} \leftarrow (\mathbf{1} - \mathbf{M}) \odot \mathbf{x}_{t-1}^{\text{pred}} + \mathbf{M} \odot \mathbf{x}_{t-1}^{\text{obs}}$ enforces the boundary condition $\mathbf{x}_o(t) \sim q_t(\mathbf{x}_o|\mathbf{x}_{data})$ while allowing \mathbf{x}_u to evolve according to the unconditional score, which we showed acts effectively as

the conditional score. Thus, in the limit of $\Delta t \rightarrow 0$, the generated samples are drawn from exact conditional distribution $p(\mathbf{x}_u|\mathbf{x}_o)$.

A.2 Details of the Scalability Test

Below are the exact system prompts used for the 20 agents in our test of the scalability on the LLM-MAS. The agents are categorized by their functional roles: **Reasoning, Bias Safety, Adversarial, and Aggregation.**

Group A: Commonsense Reasoning Specialists

Agent 1: Concept Connector

Role: Identify semantic links between entities.

You are an expert in semantic networks. Given a question and choices, identify the concept that best links the subject to the predicate based on ConceptNet relations.

[DATA]

(Input: Question + 5 Candidates)

Agent 2: Physical Interaction Analyst

Role: Analyze physical plausibility.

You focus on physical reality. Discard choices that violate laws of physics or spatial constraints. Determine which answer is physically most probable.

[DATA]

(Input: Question + 5 Candidates)

Agent 3: Social Norm Evaluator

Role: Judge social appropriateness.

You are a sociologist. Evaluate the choices based on human social norms and expected behaviors in daily situations.

[DATA]

(Input: Situation + Choices)

Agent 4: Chain-of-Thought Solver

Role: Step-by-step deduction.

Do not answer immediately. First, generate a step-by-step reasoning chain deriving the answer from the premises. Then output the final choice.

[DATA]

(Input: Question)

Agent 5: Negative Constraint Checker

Role: Elimination by impossibility.

Focus on what is NOT possible. Systematically eliminate answers that are clearly wrong or irrelevant contextually. Report the surviving option.

[DATA]

(Input: Question + Choices)

Agent 6: Analogy Mapper

Role: Solve by analogous examples.

Recall a similar real-world scenario to the one described in the question. Map the logic of that scenario to the current choices.

[DATA]

(Input: Question)

Group B: Bias Detection & Safety Critics**Agent 7: Stereotype Detector**

Role: Flag gender/racial stereotypes.

Review the proposed answer. Does it rely on harmful stereotypes regarding gender, race, or profession? If yes, flag it as UNSAFE.

[DATA]

(Input: Proposed Answer)

Agent 8: Sentiment Filter

Role: Detect toxic tone.

Analyze the emotional tone of the text. Identify any aggression, sarcasm, or mockery that biases the decision.

[DATA]

(Input: Discussion Log)

Agent 9: Cultural Inclusivity Auditor

Role: Check for Western-centric bias.

Examine if the reasoning assumes Western-centric cultural norms. Suggest alternative interpretations from non-Western perspectives.

[DATA]

(Input: Reasoning Chain)

Agent 10: Political Neutrality Bot

Role: Ensure political neutrality.

Flag any content that expresses a distinct political stance or controversial opinion not supported by facts.

[DATA]

(Input: Generated Text)

Agent 11: Protected Group Guardian

Role: Specific check for protected groups.

Specifically check for mentions of protected groups (disability, religion, age). Ensure no negative generalization is applied.

[DATA]

(Input: Text)

Agent 12: Fairness Metric Calculator

Role: Statistical bias check.

Given the distribution of answers so far, calculate if one demographic is being favored disproportionately.

[DATA]

(Input: Answer History)

Group C: Adversarial Red-Teaming**Agent 13: The Deceiver**

Role: Generate plausible wrong answers.

Your goal is to trick the voter. Generate a highly plausible but incorrect reasoning chain for one of the wrong options.

[DATA]

(Input: Question + Wrong Option)

Agent 14: Devil's Advocate

Role: Challenge the consensus.

Whatever the current majority opinion is, find a flaw in it. Argue convincingly against the leading choice.

[DATA]

(Input: Current Consensus)

Agent 15: Noise Injector

Role: Test robustness to irrelevant info.

Inject irrelevant information into the context. Check if the reasoning agents get distracted.

[DATA]

(Input: Context)

Agent 16: Corner Case Hunter

Role: Find edge cases.

Ignore the average case. Focus on extreme or rare edge cases where the proposed logic might fail.

[DATA]

(Input: Logic)

Group D: Aggregation & Decision Makers**Agent 17: Debate Moderator**

Role: Summarize different viewpoints.

Read the arguments from Agents 1-16. Summarize the conflict and identify the core point of disagreement.

[DATA]

(Input: All Agent Outputs)

Agent 18: Confidence Scorer

Role: Assign probabilities.

Rate the confidence level of the proposed answer from 0.0 to 1.0 based on the evidence provided.

[DATA]

(Input: Final Answer)

Agent 19: Meta-Voter

Role: Weighted voting.

Cast a vote for the final answer. Give higher weight to Reasoning Agents if the task is logical, and Bias Agents if the task is sensitive.

[DATA]

(Input: Task Type + Votes)

Agent 20: Final Output Formatter*Role: JSON Standardization.*

Take the final decision and format it into strict JSON: {
"id": int, "answer": str, "rationale": str }.

[DATA]

(Input: Decision)

All aforementioned templates are designed to be filled with the extracted information. Specifically, the [DATA] section serves as a dynamic interface that ingests runtime contexts—ranging from the raw input query for reasoning agents (e.g., Group A) to the intermediate debate history for the aggregation agents (e.g., Group D). Once instantiated, these prompts direct the underlying LLM to execute its designated role within a strictly defined scope. Crucially, the resulting output is automatically parsed and piped into the input slot of the subsequent agent, ensuring a coherent information flow across the communication topology derived by our sender prediction model.

A.3 Feature Selection of the Prompt Detector

To effectively infer the hidden topology of the LLM-MAS, our attacker employs a hybrid feature extraction mechanism designed to fingerprint the specific “persona” (e.g., Logician, Storyteller, Strategist) assigned to each agent. Formally, for each observed exchange, we construct a composite feature vector \mathbf{v}_t spanning three dimensions. First, we capture high-level *semantic signatures* by encoding the concatenated answer and reasoning text using a pre-trained Sentence Transformer (all-mpnet-base-v2), or alternatively via TF-IDF n-grams (1-3 word, 3-5 char) to detect role-specific vocabulary. Second, we compute explicit *stylometric statistics*, including average word length, punctuation counts, digit ratios, and uppercase ratios, to differentiate between verbose reasoning agents and concise decision-makers. Finally, uniquely to our topology inference task, we incorporate *interaction context* features, such as the current round index, the one-hot encoded identity of the *receiver*, and the receiver’s estimated degree properties (e.g., *receiver_is_hub*). These features are concatenated and fed into an ensemble of Gradient Boosting and Logistic Regression classifiers to predict the source node.

A.4 Additional Evaluation

A.4.1 Per-topology Results

A comprehensive analysis of the 200 independent test simulations in Table 6 shows that attack perfor-

mance is jointly shaped by graph topology and semantic heterogeneity among agents. From a structural perspective, centralized topologies are consistently more vulnerable than sparse ones. For example, under the CSQA dataset, the *Star* topology achieves an F1-score of 0.51, substantially outperforming the *Chain* topology (0.28). A similar trend is observed for *Complete* graphs, which attain the highest scores across datasets (e.g., F1 = 0.58 on BIAS), indicating that dense connectivity amplifies exploitable structural cues such as hub dominance and interaction asymmetry. Semantic characteristics further modulate attack efficacy. Tasks that induce distinct agent personas, including BIAS and CSQA, consistently yield higher F1-scores than more stylistically homogeneous datasets like GSM8K and FACT. In contrast, the IP Leakage baseline performs poorly across all settings, with near-zero F1-scores, demonstrating that naive identity exposure alone is insufficient for topology inference. Finally, despite variability in F1-scores across graph structures, the Mean Reciprocal Rank (MRR) remains relatively stable for CZLR (approximately 0.54–0.67), suggesting that even when top-1 identification fails, the true sender is frequently ranked among the top candidates, thereby substantially weakening sender anonymity.

A.4.2 Scalability of Model Sizes

To assess the scalability of our topology inference attack across varying backbone capabilities, we extended our evaluation to the significantly larger LLAMA-3-70B model, comparing it against the average performance of our baseline 7B–12B cluster (including Mistral, Gemma, and Phi-2). Contrary to the expectation that larger, more robust models might obfuscate leakage, our results indicate that the attack efficacy on the 70B parameter scale is consistent with, and often superior to, that of the smaller baselines. We attribute this improved vulnerability to the superior instruction-following capabilities inherent in larger models; as the model capacity increases, agents adhere more rigidly to their specific system prompts (e.g., maintaining a strict “Logician” or “Storyteller” persona). This heightened role fidelity paradoxically amplifies the stylometric and semantic distinctiveness of each node, creating sharper adversarial fingerprints that facilitate more accurate sender prediction.

Method	Data	Chain	Star	Tree	Complete	MRR
IP Leakage	CSQA	(0.00/0.00/0.00)	(0.03/0.01/0.00)	(0.00/0.00/0.00)	(0.06/0.04/0.04)	0.04
	GSM8K	(0.06/0.02/0.03)	(0.06/0.00/0.00)	(0.00/0.00/0.00)	(0.04/0.01/0.01)	0.03
	Fact	(0.00/0.00/0.00)	(0.02/0.01/0.01)	(0.06/0.02/0.02)	(0.10/0.03/0.05)	0.01
	Bias	(0.00/0.00/0.00)	(0.02/0.01/0.01)	(0.00/0.00/0.00)	(0.04/0.01/0.02)	0.04
CZLR	CSQA	(0.31/0.25/0.28)	(0.54/0.47/0.51)	(0.35/0.45/0.39)	(0.51/0.55/0.53)	0.67
	GSM8K	(0.16/0.20/0.18)	(0.41/0.40/0.41)	(0.33/0.30/0.32)	(0.34/0.33/0.33)	0.60
	Fact	(0.14/0.15/0.15)	(0.22/0.20/0.21)	(0.21/0.25/0.23)	(0.44/0.42/0.43)	0.54
	Bias	(0.32/0.40/0.36)	(0.49/0.53/0.51)	(0.20/0.20/0.20)	(0.66/0.53/0.58)	0.66
WebWeaver	CSQA	(1.00/0.98/0.87)	(0.94/0.93/0.92)	(1.00/0.90/0.83)	(0.92/0.95/0.93)	0.78
	GSM8K	(0.94/0.95/0.91)	(0.98/1.00/0.97)	(1.00/0.98/0.88)	(0.94/0.89/0.96)	0.80
	Fact	(1.00/1.00/0.89)	(1.00/0.97/0.86)	(1.00/0.90/0.85)	(1.00/0.85/0.96)	0.81
	Bias	(1.00/0.98/0.94)	(0.98/0.95/0.96)	(1.00/0.95/0.85)	(0.98/0.90/0.96)	0.89

Table 6: Graph completion performance (Precision/Recall/F1 and MRR) under different attack methods with 200 samples.

A.5 Influence on LLM-MAS performance.

A.6 Pseudocode

To facilitate reproducibility and to clearly articulate the operational mechanics of *WebWeaver*, we present detailed pseudocode for two complementary topology extraction strategies that differ in their threat assumptions and interaction capabilities. Algorithm 1 describes the *Jailbreak-based Module*, which orchestrates the attack through a structured multi-phase pipeline. This pipeline begins with offline training of a sender predictor using collected inter-agent dialogues, followed by local neighborhood identification around compromised agents. It then performs adversarial suffix optimization via gradient-based constrained generation (GCG) to elicit hidden contextual information from neighboring agents. Finally, the algorithm enters a recursive execution loop that progressively expands the inferred subgraph until the complete global topology is recovered. In contrast, Algorithm 2 formalizes the *Jailbreak-free Module*, which frames topology completion as a conditional generation problem without requiring explicit prompt manipulation. This module adopts a structural diffusion framework that iteratively infers missing edges through a reverse denoising process. To maintain structural validity, it leverages manifold-constrained fusion, ensuring that newly generated connections remain consistent with the partially observed subgraph and previously inferred relational constraints.

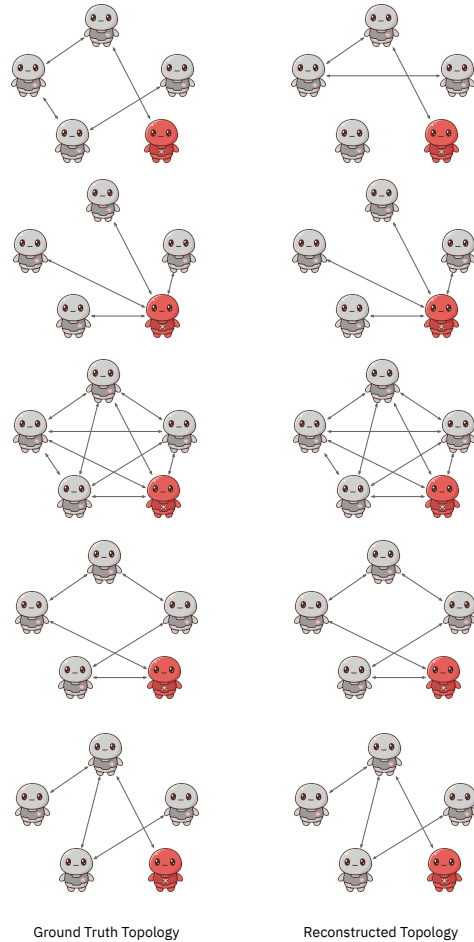


Figure 5: Inferred topology examples. All examples are selected randomly from five types of topologies. The red node stands for the compromised agent, and the gray nodes stand for the benign agents.

Algorithm 1 Jailbreak-based Module

Require: Compromised agent A_C , interaction logs \mathcal{H} , proxy LLM $\mathcal{M}_{\text{proxy}}$, propagation prompt \mathbf{x}_{prop}

Ensure: Inferred global topology \hat{G}

- 1: // Phase 1: Sender Predictor Training (Offline)
- 2: Initialize sender predictor S_θ
- 3: **for all** $(m, s) \in \mathcal{H}$ **do**
- 4: Update θ to maximize $P_\theta(\text{sender} = s \mid m)$
- 5: **end for**
- 6: // Phase 2: Local Neighborhood Identification
- 7: Initialize local adjacency $\mathbf{A}_{\text{obs}} \leftarrow \emptyset$
- 8: **while** monitoring traffic on A_C **do**
- 9: Receive message m_i
- 10: Identify sender $\hat{s} \leftarrow \arg \max_s S_\theta(m_i)$
- 11: $\mathbf{A}_{\text{obs}} \leftarrow \mathbf{A}_{\text{obs}} \cup \{(\hat{s}, A_C)\}$
- 12: **end while**
- 13: $\hat{G} \leftarrow \mathbf{A}_{\text{obs}}$
- 14: // Phase 3: Adversarial Suffix Optimization (GCG)
- 15: Initialize adversarial suffix δ
- 16: Define target response \mathbf{y} (e.g., starts with “Sure”)
- 17: **for** $t = 1$ to T **do**
- 18: Compute gradients on proxy model:
 $\nabla_{\delta_i} \mathcal{L} = \nabla_{\delta_i} (-\log p(\mathbf{y} \mid \mathbf{x}_{\text{prop}} \oplus \delta; \mathcal{M}_{\text{proxy}}))$
- 19: Select top- k token candidates based on negative gradient magnitude
- 20: Create candidate batch \mathcal{B} by substitution
- 21: $\delta \leftarrow \arg \min_{\delta' \in \mathcal{B}} \mathcal{L}(\delta') \triangleright$ Greedy update
- 22: **end for**
- 23: Set optimized prompt $\mathbf{x}^* \leftarrow \mathbf{x}_{\text{prop}} \oplus \delta$
- 24: // Phase 4: Recursive Execution & Inference
- 25: Inject \mathbf{x}^* into A_C to trigger propagation cascade
- 26: Collect forwarded histories $\mathcal{H}_{\text{global}}$ from neighbors
- 27: **for all** forwarded dialogue fragments $d \in \mathcal{H}_{\text{global}}$ **do**
- 28: Infer source/target using $S_\theta(d)$
- 29: Update global graph structure \hat{G}
- 30: **end for**
- 31: **return** \hat{G}

Algorithm 2 Jailbreak-free Module

Require: Pre-trained model ϵ_θ , observed topology \mathbf{A}_{obs} , mask \mathbf{M} , steps T

Ensure: Inferred topology $\hat{\mathbf{A}}$

- 1: Sample initial noise $\mathbf{x}_T \sim \mathcal{N}(\mathbf{0}, \mathbf{I})$
- 2: **for** $t = T, \dots, 1$ **do**
- 3: // 1. Predict denoised state for unknown regions
- 4: **if** $t > 1$ **then**
- 5: Sample $\mathbf{z} \sim \mathcal{N}(\mathbf{0}, \mathbf{I})$
- 6: **else**
- 7: $\mathbf{z} \leftarrow \mathbf{0}$
- 8: **end if**
- 9: $\mathbf{x}_{t-1}^{\text{pred}} \leftarrow \frac{1}{\sqrt{\alpha_t}} \left(\mathbf{x}_t - \frac{1-\alpha_t}{\sqrt{1-\alpha_t}} \epsilon_\theta(\mathbf{x}_t, t) \right) + \sigma_t \mathbf{z}$
- 10: // 2. Sample noisy state for known regions
- 11: Sample $\epsilon \sim \mathcal{N}(\mathbf{0}, \mathbf{I})$
- 12: $\mathbf{x}_{t-1}^{\text{obs}} \leftarrow \sqrt{\bar{\alpha}_{t-1}} \mathbf{A}_{\text{obs}} + \sqrt{1 - \bar{\alpha}_{t-1}} \epsilon$
- 13: // 3. Manifold-constrained fusion
- 14: $\mathbf{x}_{t-1} \leftarrow (\mathbf{1} - \mathbf{M}) \odot \mathbf{x}_{t-1}^{\text{pred}} + \mathbf{M} \odot \mathbf{x}_{t-1}^{\text{obs}}$
- 15: **end for**
- 16: **return** $\text{Threshold}(\mathbf{x}_0)$
